

### PRELIMINARY RESULTS OF MAPPING IRON ABUNDANCE FROM CHANG'E-1 IIM DATA

Zongcheng Ling<sup>1,2</sup>, Jiang Zhang<sup>1,2</sup>, Wenxi Zhang<sup>1</sup>, Jianjun Liu<sup>1</sup>, Guangliang Zhang<sup>1</sup>, Bin Liu<sup>1</sup>, Jianzhong Liu<sup>1</sup>  
<sup>1</sup>National Astronomical Observatories, Chinese Academy of Sciences, Beijing 100012, P.R. China, <sup>2</sup>School of Space Science and Physics, Shandong University at Weihai, Weihai, Shandong 264209, P. R. China; [zcling@sdu.edu.cn](mailto:zcling@sdu.edu.cn)

#### Introduction:

Knowledge of variability and spatial distribution of iron abundance is important for understanding the petrogenesis of lunar rocks and thus the geological history of the Moon [1]. A series of models have been developed to predict the iron abundance from Clementine UVVIS images [2-5]. Among these models, Lucey's model is the one most acceptable following with a series of refinements [5-8]. As more mission datasets (e.g., Kaguya (Japan), Chang'e-1 (China), Chandrayaan-1 (India), and LRO (United States)) [9] will be available to planetary community, it would be beneficial to compare the results from these datasets as well as to refine the algorithm of FeO mapping.

Among the 8 scientific payloads on Chang'e-1, Imaging Interferometer (IIM) is selected to detect the distribution of lunar mineral and compositions on the Moon [10]. Here we present our preliminary results to produce iron abundance map from Chang'e-1 IIM images.

#### Instrument and data overview:

Imaging Interferometer (IIM) aboard Chang'e-1 lunar orbiter is a Sagnac-based pushbroom Fourier transform imaging spectrometer. It operates from visible to near infrared (0.48-0.96  $\mu\text{m}$ ) spectral region with 32 channels at 325.5  $\text{cm}^{-1}$  spectral interval. When on orbit of 200 km above the Moon, Chang'e-1 IIM yields a ground resolution of 200m/pixel and 25.6Km swath width. IIM has got nearly 84% coverage of the Moon between 70°S and 70°N.

The data processing pipeline include dark current subtraction and relative calibration, spectrum reconstruction, radiometric calibration, photometric normalization (normalized to the standard geometry of  $i = 30^\circ$ ,  $e = 0^\circ$ ). We applied photometric normalization using a modified Lommel-Seeliger photometric model [11]. A relatively homogeneous region near Apollo 16 landing site was chosen as calibration target, and laboratory spectra of mature soil 62231 ([http://www.planetary.brown.edu/relabdocs/Apollo16\\_62231.html](http://www.planetary.brown.edu/relabdocs/Apollo16_62231.html)) was used as standard to derive the absolute IIM reflectance [12]. IIM data used in this abstract is level 2C based on the above calibrations.

#### Algorithm to derive FeO abundance:

The method for calculating the FeO abundance is similar to that of Lucey et al., 2000[5]. The first step is to acquire spectra for individual Apollo and Luna landing sampling stations from Chang'e-1 IIM data. Unfortunately, IIM missed the Apollo 15 sites, thus we could only use the rest 38 sampling sites from Table of Lucey

et al., 2000[5] to derive the algorithm of calculating FeO content.

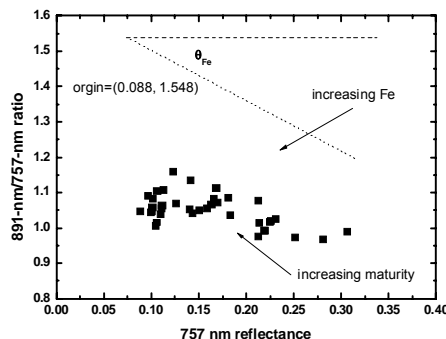


Fig. 1. NIR ratio-reflectance plot for sample-returned sites and stations observed by Chang'e-1 IIM.

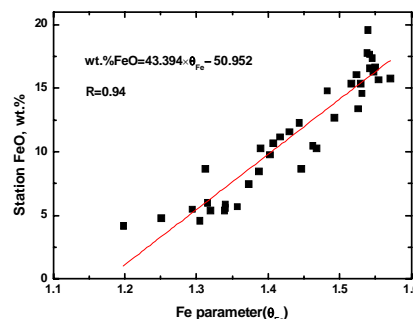


Fig. 2. FeO content of Apollo and Luna samples versus spectral iron parameter  $\theta_{\text{Fe}}$ .

The chemical content of the sampled lunar soils from Apollo and Luna missions are “ground truth” for lunar studies. We try to correlate the laboratory FeO content of typical lunar soils from lunar landing sites with the remotely sensed image data. The spectral data for 38 sample returns sites and stations extracted from Chang'e-1 images were plotted on a ratio reflectance diagram as shown in Fig. 1. The key is in calculations to suppress the maturity effect by an angle named Fe sensitive parameter  $\theta_{\text{Fe}}$ , which would have a linear relationship with FeO abundance. By maximizing the correlation between remotely measured  $\theta_{\text{Fe}}$  and FeO content, we got the “hypermature” endmember located at (0.088, 1.548).

We got the expression of  $\theta_{\text{Fe}}$  as

$$\theta_{\text{Fe}} = -\arctan\left(\frac{R_{891}/R_{757} - 1.548}{R_{757} - 0.088}\right)$$

The plot of station FeO content and spectral iron parameter is shown in Fig. 2. The equation of best fit for

these data points is

$$\text{wt. \% FeO} = \theta_{\text{Fe}} \times 43.394 - 50.952$$

This equation has a correlation coefficient of 0.94. The scatter of the data points about the polynomial fit yield a standard deviation of 1.58 wt % FeO.

#### Case Regional study:

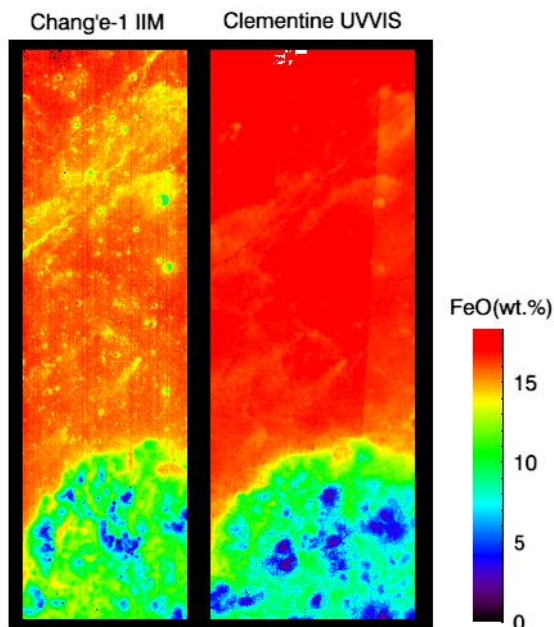


Fig.3. Comparisons of iron abundance map between Chang'e-1 IIM and Clementine UVVIS image.

Based on our model and the algorithm by Lucey [5], we produced a strip of iron map near the southern rim of Mare Crisium (as shown in Fig. 3).

When we compare these results with what was obtained by Lucey's model, we find similarities and good correlation between these two images. However, Chang'e-1's data seems to show iron poorer with more detailed features in the mare regions, while iron richer in the highland regions. The average FeO content difference between these two images is 0.51 wt % (for IIM is 14.07 wt %, for UVVIS is 14.58 wt %). The distribution of respective data points is shown in Fig.4. The bimodal distribution is in relation with mare and highland regions. The major mare soils FeO are between 16-17 wt %, while Chang'e-1 data exhibits a peak at around 15 wt %. Conversely, Chang'e-1 data have higher iron content (11 wt %) in highland as compared to Clementine data (8-9 wt %).

The discrepancies of FeO content between these two images may be from complex sources. First, the absolute reflectance spectra of IIM data used in these calculations show lower S/N than that of Clementine. Second, due to the poor quality of 918 and 947 nm images, we choose band 891nm for the regression calculations(not

the 950nm by Lucey [5]), which may decrease the sensitivity of this model. In addition, considering the two images have different solar incidence directions, topographic shading effect may be potential causes for the FeO content difference, especially for highland regions.

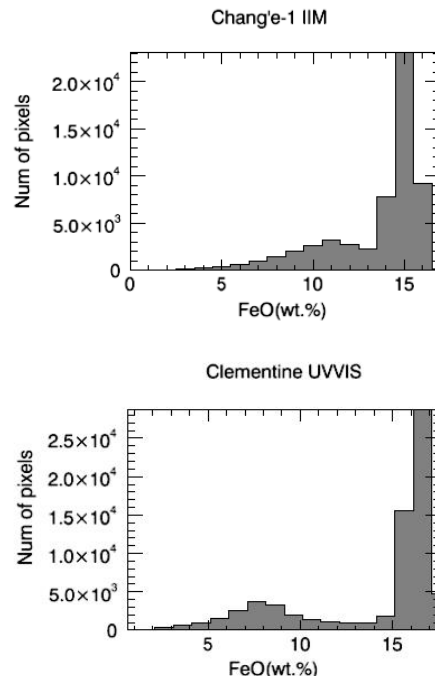


Fig.4. Data distribution of Chang'e-1 IIM and Clementine UVVIS images.

#### Conclusions and future work:

As compared with Clementine UVVIS images, IIM datasets from Chang'e-1 satellite also exhibit the potential to extract FeO abundance distributions on the Moon. However, preliminary model results suggest an underestimate ( $\sim 2$  wt %) of FeO content for mare region, while an overestimate ( $\sim 3$  wt %) for highland region.. For future work, we will continue the analysis for origin of this discrepancies and uncertainties of this algorithm to improve FeO model for IIM data.

**Acknowledgements:** This study is supported by China Postdoctoral Science Foundation (No.20090450580) and the Young Researcher Grant of National Astronomical Observatories, Chinese Academy of Sciences.

**References:** [1] Taylor et al. (1987) *GCA*, 51, 1297-1309. [2] Lucey et al. (1995) *Science*, 268, 1150-1153. [3] Blewett et al. (1997) *JGR*, 102, 16319-16325. [4] Lucey et al. (1998) *JGR*, 103, 3679-3699. [5] Lucey et al. (2000) *JGR*, 105, 20297-20305. [6] Lawrence, et al. (2002) *JGR*, 107(E12), 5130. [7] Gillis, et al. (2004) *GCA*, 51, 1297-1309. [8] Wilcox et al. (2005) *JGR*, 110, E11001. [9] Pieters et al., (2008) *Adv Space Res*, 42, 248-258. [10] Zheng, et al. (2008) *Planet Space Sci*, 56, 881-886. [11] Hillier et al. (1999) *Icarus*, 141, 205-225. [12] Pieters, (1999) *Workshop on New Views of the Moon 2: Understanding the Moon Through the Integration of Diverse Datasets*, 47.